ELSEVIER

The thermal degradation of bisphenol A polycarbonate in air

Bok Nam Jang, Charles A. Wilkie*

Department of Chemistry, Marquette University, P.O. Box 1881, Milwaukee, WI 53233, USA

Abstract

The thermal degradation of polycarbonate in air was studied as a function of mass loss using TGA/FTIR, GC/MS and LC/MS. In the main degradation region, 480–560 °C, the assigned structures of smaller molecules and linear molecules that evolved in air were very similar to those obtained from the degradation in nitrogen; the degradation of polycarbonate follows chain scission of the isopropylidene linkage, in agreement with the bond dissociation energies, and hydrolysis/alcoholysis of carbonate linkage. Compared to the degradation in nitrogen, some differences were observed primarily in the beginning stage of degradation. Oxygen may facilitate branching as well as radical formation via the formation of peroxides. These peroxides undergo further dissociations and combinations, producing aldehydes, ketones and some branched structures, mainly in the beginning stage of degradation. It is speculated that the intermediate char formed in the beginning due to branching reactions of peroxide interferes with the mass transfer through the surface of degrading polycarbonate in the main degradation. Thus, even though the mass loss begins earlier in air, a slower mass loss rate is observed.
© 2004 Elsevier B.V. All rights reserved.

Keywords: Bisphenol; Thermal degradation; Isopropylidene linkage; Peroxides

1. Introduction

Bisphenol A polycarbonate (PC) has attracted considerable attention, since PC is one of the most widely used engineering polymers and it shows very good mechanical and thermal properties. In addition, PC itself exhibits flame retardancy and produces a large fraction of char upon combustion [1]. Polycarbonate and its blends exhibit excellent fire retardant performance with conventional halogen or halogen-free fire retardants [2,3]; it is thought that this behavior relates to the degradation characteristics of polycarbonate. The degradation behavior of a polymer is closely related to its flame retardancy and, in order to achieve effective flame retardancy, it is a prerequisite that the degradation pathway of the polymer be well understood [4].

Lee studied the thermal degradation of polycarbonate in vacuum and in an oxygen atmosphere. He suggested that the initial step is oxidative hydrogen cleavage from the iso-

propylidene linkage and then carbon–carbon bond scission, followed by hydrolysis and alcoholysis of the carbonate. Various evolved products were assigned up to a molecular weight of 228 using mass spectroscopy [5].

Davis et al. assigned CO_2, phenol and bisphenol A as the main volatile products, together with a small amount of CO, alkyl phenols and diphenyl carbonate. They speculated that the carbonate group undergoes rearrangements, along with hydrolysis and alcoholysis; they also proposed the formation of a xanthone unit during thermal degradation of PC [6–8].

McNeill et al. investigated the thermal degradation mechanism of PC using thermal volatilization analysis (TVA) in nitrogen. They assigned some cyclic oligomers of bisphenol A carbonate and various phenol structures having masses less than 228 using GC/MS and suggested a homolytic chain scission mechanism for the degradation of PC [9,10].

Montaudo et al. carried out an extensive study on the degradation of polycarbonate with pyrolysis-GC/MS [11,12], direct pyrolysis mass spectral (DPMS) measurements [13] and MALDI-TOF investigations [14–16]. In the PGC/MS and DPMS study, they assigned xanthone units as well as

* Corresponding author. Tel.: +1 4142887239; fax: +1 4142887066.
  E-mail address: charles.wilkie@marquette.edu (C.A. Wilkie).

cyclic oligomers, and proposed that the major degradation pathways for PC include the rearrangement of carbonate linkage by intramolecular ester exchange and disproportionation of isopropylidene linkages.

Since there is little work done on the PC degradation mechanism at atmospheric pressure, we have used TGA/FTIR, GC/MS and LC/MS to study the degradation of PC in nitrogen and have assigned the structures for many significant evolved products and suggested that thermal degradation of PC in nitrogen occurs by chain scission of the isopropylidene linkage, and hydrolysis/ alcoholysis and decarboxylation of carbonate linkage [17]. The xanthone units and cyclic oligomers were not detected among the evolved products in this study in nitrogen.

Most of the above results were obtained under nitrogen or vacuum. However, the degradation behavior upon heating or combustion may be altered in the presence of oxygen. Montaudo et al. analyzed the soluble solid fraction of thermally oxidized PC by heating at 300 and 350 °C in air for up to 180 min and suggested its oxidation pathway to be radical formation by peroxy and subsequent rearrangements producing biphenyl linkages, etc. [18]. They did not report the presence of xanthone units in air. It is generally believed that the presence of oxygen accelerates radical formation during heating or photo irradiation [19]. However, the involvement of oxygen in the thermal degradation of the polymer during combustion is not clear. Although the environment of the decomposing sample may affect the degradation pathway, it has been said that in the case of combustion, there may be no oxygen effect during combustion because oxygen is not present with the degrading polymer [20,21].

In order to investigate the thermal degradation behavior of polycarbonate under an air atmosphere, TGA/FTIR was performed in air. To obtain molecular structure information on the fragments produced during the degradation, the evolved products were collected at each mass loss and analyzed using FTIR, GC/MS and LC/MS. The solid residues after degradation were analyzed using FTIR.

2. Experimental

2.1. Materials

PC samples were provided by Cheil Industries Inc., and were used as received; this material is end-capped with *t*-butyl phenol in order to further improve the thermal stability. The number and weight average molecular weight of the bisphenol A polycarbonate are 16,000 and 28,000, respectively.

2.2. TGA/FTIR analysis and sampling of evolved products

TGA/FTIR was carried out at a heating rate of 20 °C/min and a gas flow of 60 ml/min on Cahn TG 131 instrument which was connected to Mattson Research grade FTIR through stainless steel tubing. This instrument uses a sniffer tube that extends into the sample cup to remove the evolved gases; this sniffer tube removes gas at the rate of 40 ml/min. The evolved volatile products are introduced into the IR chamber through the sniffer and analyzed by vapor-phase FTIR. The temperature reproducibility of the TGA is ± 3 °C and the fraction of non-volatile is $\pm 3\%$. The sample size was 40–60 mg. The evolved products during thermal degradation were collected for 5–20 min as a function of mass loss using a cold trap at a temperature of -78 °C.

2.3. Analysis of evolved condensable products at each mass loss

The collected-evolved products in the sniffer and cold trap were washed with acetonitrile. FTIR (Nicolet Magna 560 Model) analysis was performed by placing the material on a KBr window and allowing the solvent to evaporate. GC/MS spectra were obtained using an Agilent 6850 series GC connected to an Agilent 5973 Series MS (70 eV electron ionization). LC/MS spectra (Electrospray Ionization, negative) were obtained using an Agilent 1100 Model.

2.4. FTIR Analysis of solid residue sample

The solid residues at each mass loss were collected and analyzed by FTIR (Nicolet Magna Model 560).

3. Results and discussion

3.1. Thermal degradation temperature and in situ FTIR results

The TGA curve of bisphenol A polycarbonate under an air atmosphere at the rate of 20 °C/min is shown in Fig. 1; the TGA result in nitrogen is also included. In comparison with degradation in nitrogen, mass loss in air begins at 450 °C, which is about 50 °C earlier than in nitrogen. The end of the main degradation step occurs at about 560 °C in both cases, leaving a residual mass of about 35%. It has been noted that the mass loss rate in air is slower than that in nitrogen in the main mass loss region. The residue remains constant up to 700 °C in nitrogen, but it continues to degrade in air, eventually going to zero.

Fig. 2 shows the in situ FTIR spectra of the evolved products at each mass loss stage. At the beginning of mass loss, CO_2 evolution, 2200–2400 cm^{-1}, was significant and the characteristic bands of substituted phenol derivatives were observed. The weak noise-like bands at 1400–1900 cm^{-1} and 3500–3900 cm^{-1} were due to H_2O evolution. The generation of CO_2 and H_2O was observed over the whole mass loss range. Peaks due to free alcohol, 3645 cm^{-1}, sp^2 carbon–hydrogen and sp^3 carbon–hydrogen stretching, respectively, above and below 3000 cm^{-1}, as well as carbonyl stretching of the carbonate functional group, 1780 cm^{-1},
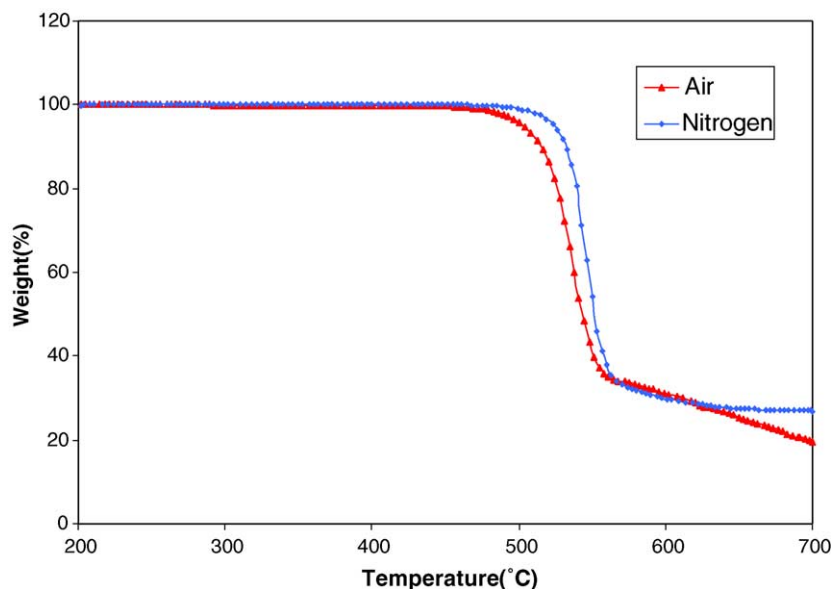
Fig. 1. Thermogravimetric analysis curves for Bisphenol A Polycarbonate at a heating rate of 20 °C per minute in nitrogen and air.

were observed. The band at $1690\,cm^{-1}$, for the low-mass loss region, corresponds to a ketone functional group. The peaks at $1610\,cm^{-1}$ and $1510\,cm^{-1}$ are due to ring stretching of phenyl compounds, and the range between 1300 and $1150\,cm^{-1}$ corresponds to the carbon–oxygen stretching region of ethers and carbonates. The bands at $1880\,cm^{-1}$ and $830\,cm^{-1}$ are overtones and out-of-plane deformations of *para*-disubstituted aromatic compounds.

The bands in the $2800–3200\,cm^{-1}$ region, which is C–H stretching, show qualitative changes as mass loss proceeds. Initially, a relatively strong sp^3 carbon–hydrogen peak was observed in the low-mass loss region, and then sp^2 C–H bands became the major peaks at the high-mass loss region. In the case of low-mass loss region, less than 20%, two carbonyl stretching peaks at 1780 and $1690\,cm^{-1}$ were clearly observed, suggesting the presence of different carbonyl functional groups. In the high-mass loss region, the carbonyl peak of carbonate at $1780\,cm^{-1}$ is still present and the other car-

bonyl group band, $1690\,cm^{-1}$, became very small. With the exception of the beginning stage of mass loss, the FTIR spectra at high-mass loss were almost identical to those obtained in a nitrogen atmosphere. From the TGA and FTIR results, it can be speculated that the presence of oxygen accelerates the degradation of polycarbonate, leading to evolution of ketones in the low-mass loss region.

3.2. Analysis of collected products evolved at each mass loss

The evolved products were collected as a function of mass loss and FTIR spectra for the condensed products, after evaporating the solvent, as shown in Fig. 3. The spectra may be divided into two regions based on the characteristic functional groups seen in the FTIR results: the low-mass loss region, 0–20%, and the high-mass loss region, 20–70%, that corresponds to the main degradation.

There is no qualitative difference in the functional groups that were observed in the main mass loss region (over 20% mass loss) and the peaks were very similar to those in nitrogen, except for the beginning stage of degradation. In the low-mass loss region, two carbonyl peaks, at 1750 and $1660\,cm^{-1}$, are observed, which implies another carbonyl group in addition to carbonate. In nitrogen, the only carbonyl band that was observed was carbonate. The carbonate peak, $1750\,cm^{-1}$, was observed over the whole mass loss range in air, and the carbonyl peak around $1660\,cm^{-1}$ in the low-mass loss region, which was not observed in nitrogen, corresponds to a ketone functional group. It is thought that the 1780 and $1690\,cm^{-1}$ in the vapor-phase FTIR shifted to 1750 and $1660\,cm^{-1}$ in the condensed-phase FTIR, due to hydrogen bonds between carbonyl groups and alcohols, whose structures will be shown in Table 1. The intensities of these carbonyl bands are rela-
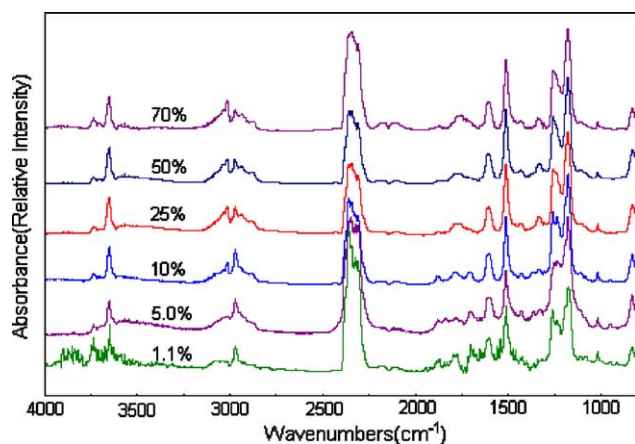

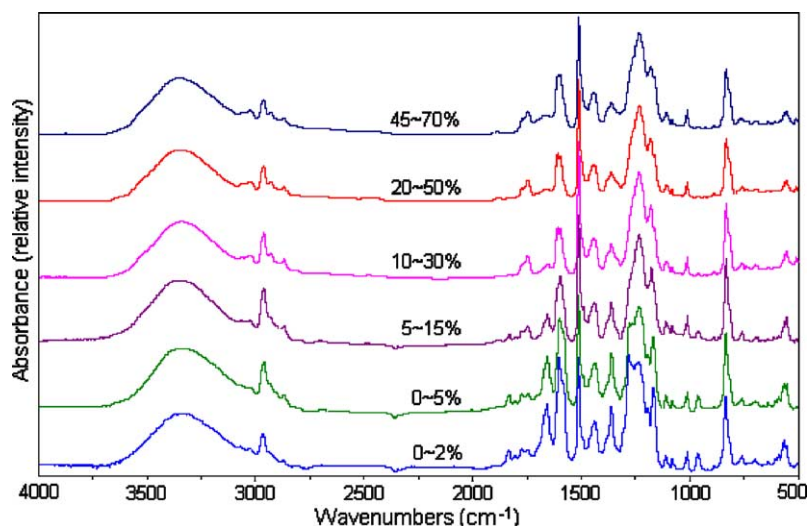Fig. 2. Vapor-phase FTIR of polycarbonate with mass loss in air.

Fig. 3. Condensed-phase FTIR for evolved products at each mass loss region.

tively low, because the most abundant evolved products are alkyl substituted phenols and bisphenol A, as can be seen in the GC/MS result (Fig. 4 and Table 1). The bands between 1150 and 1300 cm^{-1} are due to the carbon–oxygen stretching of ethers and carbonates. Again, the bands at 830 cm^{-1} and 1880 cm^{-1} indicate that the evolved products are mainly *para*-disubstituted benzenes. In short, the FTIR spectra suggest that there were considerable amounts of alcohols, ethers

and carbonates in the evolved products over the whole mass loss range, along with some ketones only in the low-mass loss region. Hence, the primary differences in degradation behavior between nitrogen and air occur at the beginning of the degradation.

In order to provide an opportunity for the identification of the components in the evolved products, both GC/MS and LC/MS were used; the strategy that was followed was to use

Table 1
Assigned structures having one and two benzene rings from GC/MS results

Group	Structure (*m/z*, retention time in minutes)
Alcohols	HO⟨⟩ (94, 9.7), HO⟨⟩–CH₃ (108, 11.6), HO⟨⟩–C₂H₅ (122, 13.3), HO⟨⟩–C₂H₃ (120, 14.1), HO⟨⟩–C₃H₇ (136, 14.3), HO⟨⟩⟨ (150, 15.3), HO⟨⟩–C₃H₅ (134, 15.5), ⟨⟩⟨⟩–OH (212, 22.7), HO⟨⟩⟨⟩–OH (214, 25.4), HO⟨⟩⟨⟩–OH (228, 25.9)
Aldehyde ketones	HO⟨⟩–C(O)–H (122, 16.4), HO⟨⟩–C(O)–CH₃ (136, 17.5), H₃C⟨⟩–O–C(O)–O–⟨⟩–C(O)–CH₃ (270, 28.3)
Ethens	H₃C⟨⟩–O–⟨⟩–CH₃ (198, 19.9), H₃C⟨⟩–O–⟨⟩–C₂H₅ (212, 20.5), H₃C⟨⟩–O–⟨⟩–C₂H₃ (210, 21.3), C₂H₅⟨⟩–O–⟨⟩–C₂H₅ (226, 23.7)
Carbonates	H₃C⟨⟩–O–C(O)–O–⟨⟩ (228, 22.2), H₃C⟨⟩–O–C(O)–O–⟨⟩–CH₃ (242, 23.5), C₂H₅⟨⟩–O–C(O)–O–⟨⟩–CH₃ (256, 24.5), H₃C⟨⟩–O–C(O)–O–⟨⟩–C₂H₃ (254, 24.8), C₂H₅⟨⟩–O–C(O)–O–⟨⟩–C₂H₅ (270, 25.2), C₂H₅⟨⟩–O–C(O)–O–⟨⟩–C₂H₃ (268, 25.7), C₂H₅⟨⟩–O–C(O)–O–⟨⟩–C₃H₇ (284, 26.2), C₂H₃⟨⟩–O–C(O)–O–⟨⟩–C₃H₇ (282, 26.7), C₃H₇⟨⟩–O–C(O)–O–⟨⟩–C₃H₇ (298, 27.0), C₄H₉⟨⟩–O–C(O)–O–⟨⟩–C₄H₉ (326, 28.7)

GC/MS for lower molecular weights, and to reserve LC/MS for higher molecular weights. Since the GC and LC traces exhibit relative abundance of the evolved products and its sensitivity to compounds is proportional to ionization efficiency, the following results are primarily explained by comparing GC and LC traces and using the relative intensities as an indicator of changes in composition.

The GC trace, as a function of mass loss at which the sample was collected, shown in Fig. 4, has appended to it the molecular weights that have been discerned, and the corresponding structures having one or two benzene rings were identified, using the mass fragmentation pattern and functionality information from FTIR, as shown in Table 1. For the products having two benzene rings, the evolved products contain mainly ether and carbonate linkages with some ketone and aldehyde structures.

In the beginning degradation stage, the evolution of *t*-butyl phenol (*m/z* 150, 15.3 min), which has been used to end-cap the end of polycarbonate chain, and *m/z* 326 (28.7 min), bis(*t*-butyl phenyl)carbonate, were noted, which means scission at the chain-ends of polycarbonate. The ether compounds, *m/z* 212 (20.5 min) and *m/z* 210 (21.3 min) are also assigned, which implies decarboxylation of carbonate linkage as will be shown in Scheme 3.

It was proposed that the main degradation pathway of polycarbonate in nitrogen follows chain scission of the iso-
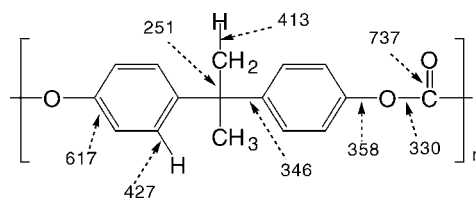
Fig. 5. Bond dissociation energy of bisphenol A polycarbonate in kJ/mol [5,24].

propylidene linkage according to bond dissociation energies as shown in Fig. 5, and hydrolysis/alcoholysis and decarboxylation of carbonate linkages, since the carbonate linkage easily undergoes reaction with H_2O and alcohols at elevated temperature [17]. This is generally in agreement with the work of Lee [5] and McNeill [9,10]. It appears that the intense peaks of bisphenol A over the whole mass loss range were mainly caused by hydrolysis or alcoholysis of carbonate linkages rather than chain scission.

Compared to the results in nitrogen, some differences were observed in the beginning stage of degradation, both from the GC traces and the FTIR results; the *m/z* value of 122 (16.4 min), 136 (17.5 min) and 270 (28.3 min) were not seen in nitrogen but are present in air, and bisphenol A (*m/z* 228, 25.9 min) was significant even in the beginning mass loss region, which suggests hydrolysis/alcoholysis of carbonate linkage. The *m/z* 122 (16.4 min) corresponds to *p*-hydroxybenzaldehyde. The *m/z* value of 136 (17.5 min), which was assigned as *p*-hydroxyacetophenone through the fragment pattern and confirmed by co-injection, may arise via methyl scission of isopropylidene linkage followed by peroxide formation and β-scission [22] of alkoxy radicals, as shown in Scheme 1. Elimination of the aryl group in alkoxy radicals via β-scission is much more favorable than that of methyl or hydrogen producing ketones and phenyl radicals [22]. The phenyl radicals, which are produced in Scheme 1, may be used as the reaction source in Scheme 2, which also presents the degradation scheme for the low-mass loss region. The carbonyl groups of *m/z* 122 (16.4 min), 136 (17.5 min) and 270 (28.3 min) have vibration modes at around $1660 \, cm^{-1}$ [23], which are present in the FTIR results for low mass region (Fig. 3). Some other acetophenone structures were identified by Montaudo et al. in the analysis of the soluble fraction of thermally oxidized polycarbonate [18].

Scheme 1, which covers the initial mass loss stage, supports the presence of ketones in the evolved products and some important features of degradation pathway of polycarbonate: first, the evolution of relatively large amounts of CO_2 and H_2O in the low-mass loss region in air can be explained by this scheme; second, the significant evolution of bisphenol A at the beginning stage of degradation is caused by the hydrolysis of the carbonate linkage by water, which is produced in this scheme; and third, this degradation scheme suggests that methyl scission of isopropylidene linkage occurs first [17], which is in agreement with the bond dissociation energies as shown in Fig. 5.
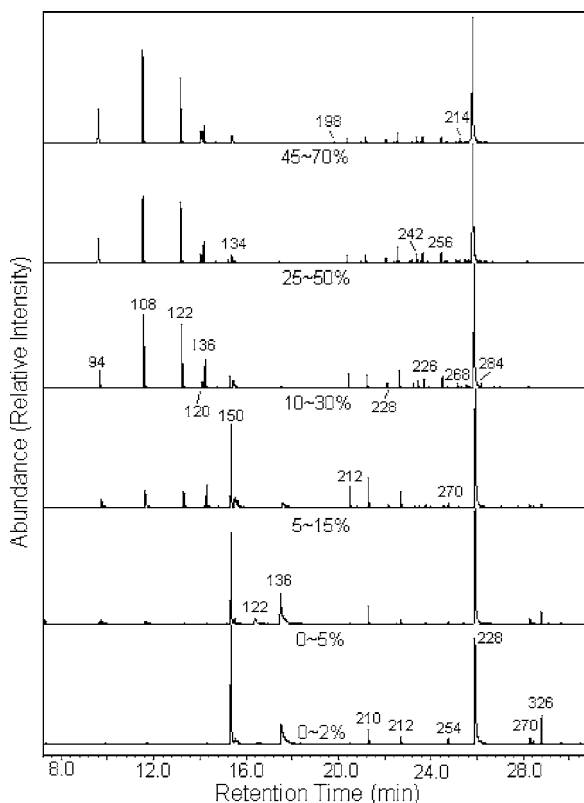

Fig. 4. GC traces of the evolved decomposition products. Inset numbers on each peak indicate the molecular weight acquired by mass spectroscopy and percentages denote the mass loss range for the collected sample.

The structure of the ketone at m/z 270 (28.3 min) can arise through the isopropylidene scission, as shown in Scheme 1; the structures of the compound with a phenyl end group (m/z 256), an ethyl end group (m/z 284) and an isopropyl end group (m/z 298), with the same skeletal structure and which are not observed in significant amounts, can also arise via chain scission at the isopropylidene linkage. This result is consistent with the relative intensity trend of phenol (m/z 94, 9.7 min), p-methylphenol (m/z 108, 11.6 min), p-ethylphenol (m/z 122, 13.3 min) and p-isopropylphenol (m/z 136, 14.3 min), which shows the most abundant intensity for p-methylphenol in the GC traces, implying chain scission following the bond dissociation energies. Comparing the relative intensities of the structures for m/z 122 (16.4 min), m/z 136 (17.5 min) and m/z 270 (28.3 min) produced via Scheme 1 in the GC traces of the low-mass loss region with those of the main loss region, it appears that the oxygen effects are primarily observed in the beginning stages of degradation (0–20% mass loss region), since the oxygen in the atmosphere mainly affects the surface of degrading polymer. The FTIR results of Figs. 2 and 3 support this.

The GC/MS results for the main mass loss region (over 20% mass loss) are qualitatively very similar to those in nitrogen. Thus, the evolved products are very similar to the results in nitrogen, which means the same degradation pathway in the case of the main degradation stage. It has been proposed that the presence of 1,1′-bis(4-hydroxyphenyl)ethane (m/z 214, 25.4 min) suggests that methyl scission occurred and may be the source of branched compounds in the evolved products in nitrogen [17]. However, this peak was observed with a relatively small intensity in the evolved products in air, which means that more branched structures were formed in air. From the TGA curves of Fig. 1, it was observed that the mass loss rate in air is slower than that in nitrogen. It is likely that the presence of oxygen during thermal degradation accelerates the branching reactions on the surface of degrading polycarbonate at the beginning of the degradation and forms an insulating surface layer. Therefore, diphenylethyl radicals, which are formed in the condensed phase via methyl scission of the isopropylidene group, may have more chance to undergo reaction with other radicals and form branched structures in condensed phase, as will be shown later in Schemes 2 and 5.

Fig. 6 shows and assigns the longer retention time, and hence higher molecular weight, materials from the GC/MS
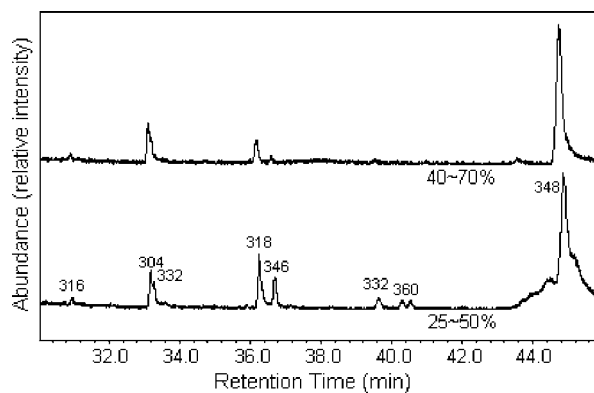

Fig. 6. Expanded GC traces for higher retention time.

trace for the main mass loss region. The assigned structures correspond to the structures having three benzene rings as shown in Table 2. Most structures are classified as either ethers or carbonates. It is notable that the relative abundance of m/z 348 (44.8 min), carbonate, is more intense than that of m/z 318 (36.2 min), ether, which is the opposite result to that in nitrogen. Thus, the shift from the ether-containing group to a branched structure is more probable in the main degradation because of the intermediate surface char layer which was formed at the initiation of the degradation. The branched structures were not significant in GC traces, probably because of their size and volatility, and these will be shown in the LC/MS results.

Fig. 7 shows the LC/MS results which have a molecular weight range of 250–800. While the assignment of structures having one, two and three benzene rings in GC/MS is fairly easy and clear, it is much more complicated to assign the structures for the higher molecular weights that are obtained by LC/MS, because there are many possible isomers and only molecular weights, with no fragment patterns, are available.

In order to simplify and assign the significant peaks for high molecular weights in the LC/MS data, several postulates were developed based upon the GC/MS and FTIR data and previous work [17]. First, the possibility of unsaturated aliphatic end groups was discarded by a comparison of the relative abundance of m/z 122 (13.3 min) and m/z 136 (14.3 min), which have saturated aliphatic end groups, with the unsaturated analogues at m/z 120 (14.1 min) and m/z 134 (15.3 min) in Fig. 4. Second, according to the bond

Table 2
The structures having three benzene rings in GC/MS results of Fig. 5

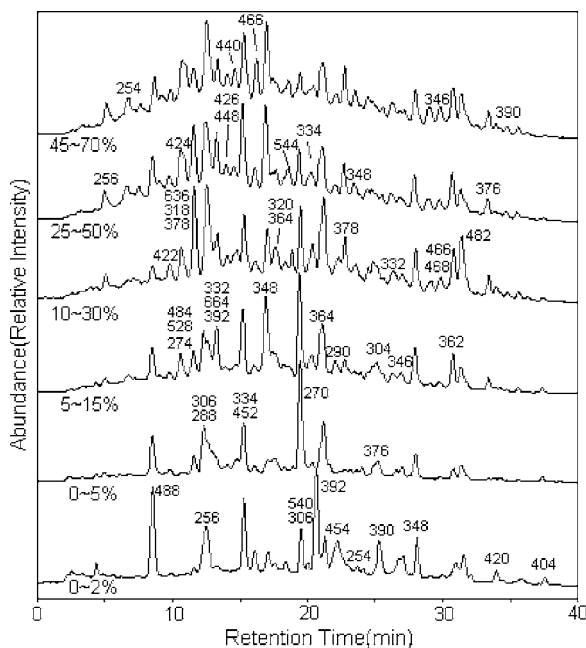| Linkage	Structures (m/z, retention time in minutes)
Ethers	(304, 33.0), (318, 36.2), (332, 39.5), (316, 30.8)
Carbonates	(332, 33.1), (346, 36.6), (360, 40.4), (348, 44.8)

Fig. 7. LC/MS results for the evolved condensed products at each mass loss. Inset numbers indicate the molecular weight acquired by mass spectroscopy.

dissociation energies [24], the abundance of products having methyl or ethyl substituents on the benzene ring is larger than those with hydrogen or isopropyl. Third, all benzene rings are para disubstituted based on FTIR data. Fourth, in those cases where several isomers appear possible and/or a linear structure seems unlikely, branched structures based on 1,1-bis(4-hydroxyphenyl) ethane were considered. In accordance with these postulates and the GC/MS results, the significant peaks from LC/MS were speculatively assigned as shown in Table 3.

For the structures having two or three benzene rings in the LC/MS, some structures which have been already assigned by the GC/MS are not repeated here. In comparison with the results in nitrogen, many carbonate and ether containing structures were again assigned while some ketones and aldehydes were mainly found in the low-mass loss region, but overall, more branched structures were identified. The evolved products due to the thermal degradation of polycarbonate in the presence of oxygen showed some results different from those in nitrogen; for instance, ketone and aldehyde, which were not observed in nitrogen, are seen at *m/z* 376 (25.1 min) and 390 (26.7 min) and these may arise in a fashion similar to that shown in Scheme 1, especially in the low-mass loss region, and many branched structures were formed via radical recombination over the whole mass loss range.

In the case of the linear structures having four benzene rings, the number with significant abundance was reduced as compared to the degradation results in nitrogen, while more branched structures were assigned in air. Thus, as described in the GC/MS results, the LC/MS results also support the notion that the presence of oxygen accelerates the formation of branched structures on the surface in the beginning stage of degradation as shown in Scheme 2, and it may provide a thermal barrier for the degrading polycarbonate by forming this surface layer, which gives more chances for degrading substances not at the surface to undergo branching reactions. This explains why the mass loss rate is slower in the presence of oxygen, even though the mass loss initiation temperature is earlier than in nitrogen (Fig. 1).

As the molecular size of the evolved products increases, branched structures are more probable than linear structures. One of the new peaks is *m/z* 488 (8.7 min), which was significant in the low-mass loss region, implying that this compound was produced due to the presence of oxygen. It can be assigned to a structure having an ether linkage due to peroxide formation in the presence of oxygen, as shown in Scheme 2. The source of phenyl radical combining with alkoxy radical might come from Scheme 1, which was produced via β scission of alkoxy radical. In the case of the structure of *m/z* 488, even though it was mainly formed in the beginning stage of degradation, it is seen to the end stage of the degradation. Therefore, it may be concluded that peroxide structures are formed in air and those structures undergo dissociation and radical combination at the peroxide site, producing aldehydes, ketones and branched structures.

3.3. FTIR analysis of solid residues at each mass loss

FTIR spectra of the solid residues at each mass loss are shown in Fig. 8. The alcoholic peaks, $3500\,cm^{-1}$, were observed over the whole mass loss range, and the characteristic peak of carbonate, $1780\,cm^{-1}$, could be observed up to 50% mass loss and then disappeared at 70%. This means that carbonate groups are stable even at very high temperatures. The bands around $1200\,cm^{-1}$ correspond to the carbon–oxygen stretching region. The FTIR of the solid residues in air were very similar to those in nitrogen.

The relative intensity changes of carbon–hydrogen stretchs can give some information on the source of hydrogen abstraction for the evolved products during degradation, since it is thought that the hydrogen source should be from the condensed phase. The relative intensity of both sp^2 carbon–hydrogen and sp^3 carbon–hydrogen around $3000\,cm^{-1}$ are variable. Considering the bond dissociation energies, as shown in Fig. 5, it may be that hydrogen abstraction occurs first from the aliphatic carbon–hydrogen and then from the aromatic carbon–hydrogen. However, the dissociation energies are not very different and hydrogen can be abstracted from both aliphatic and aromatic sites. It is likely that the radical produced by hydrogen abstraction in the condensed phase is so unstable that it may instantly form a branched structure or induce carbonization. The chemistry in the condensed phase of the polycarbonate during thermal degradation is not clear because of the difficulty and complexity of analyzing the residues produced in the degradation.

Table 3
Structure assignments for the significant peaks in LC/MS

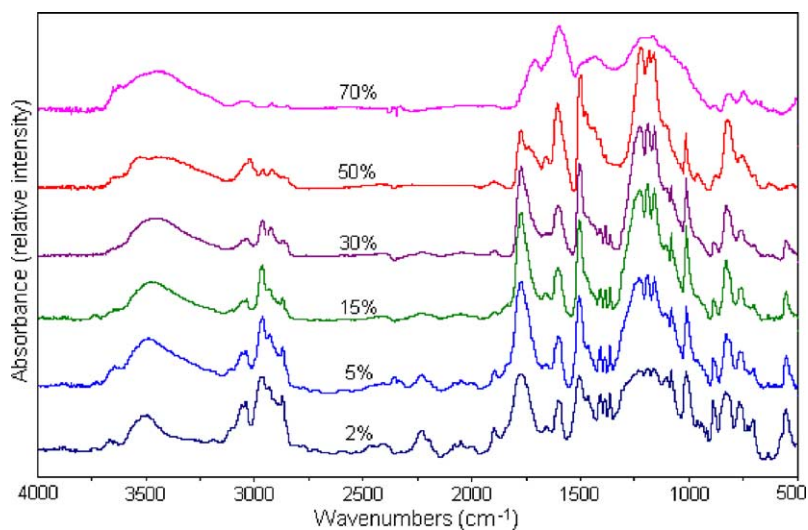| Group	Structures (*m/z*, retention time in minutes)
Three rings	
Four rings	
Branch	

Fig. 8. FTIR spectra for solid residues at each mass loss.

3.4. Thermal degradation pathways of polycarbonate in air

The thermal degradation mechanisms for bisphenol A polycarbonate are suggested as shown in Schemes 1–5, based on the analysis of the evolved products during thermal degradation of bisphenol A polycarbonate in air.

Schemes 1 and 2 primarily correspond to the initial stage of degradation; in the beginning stage of degradation, since no significant mass loss is exhibited, the relative concentration of oxygen on the surface of degrading polymer may be high and it is possible for oxygen to react with the degrading polymer and form peroxide. Aldehydes and ketones are evolved via Scheme 1, along with H_2O and phenyl radicals. The H_2O produced in Scheme 1 induces hydrolysis of the carbonate linkage, which mainly produces bisphenol A and CO_2. As shown in the vapor-phase FTIR results (Fig. 2), relatively intense bands due to CO_2 and H_2O support Scheme 1, while the phenyl radicals produced in Scheme 1 may be involved in the formation of branched structures, as shown in Scheme 2. Scheme 2 shows an example how oxygen may induce branching on the surface of degrading polycarbonate. This assists in the formation of an intermediate surface char layer which prevents the access of oxygen and the evolution of degraded smaller molecules. Through Scheme 1 and 2, it is thought that oxygen also facilitates the formation of the branched structures on the surface of degrading polycar-

bonate as well as radical formation which may initiate mass loss.

Therefore, in the case of main degradation stage (over 20% mass loss in TGA curve), due to the intermediate surface layer and relatively fast mass loss rate of degrading polycarbonate, the effect of oxygen becomes negligible. Hence, many of the evolved products are the same as those in nitrogen; it appears that the degradation pathway in this region in air is similar to that in nitrogen. Schemes 3–5 are the degradation pathways of main degradation region. As described in the section on GC/MS, the primary evolved products in the main degradation region are phenol, alkyl phenols, bisphenol A, ethers and carbonates. In the case of the ether linkage, it was suggested that the ether linkage is thermally produced through a Kolbe–Schmitt type rearrangement of carbonate [16,18,25,26] or through the concerted 1,3-shift of carbonate group [5], followed by decarboxylation, as shown in Scheme 3.

Most of the evolved products in this main degradation stage are thought to be produced through the chain scission of the isopropylidene linkage and hydrolysis/alcoholysis of the carbonate linkage, producing alkyl, phenyl and alcohol ends for the structures having two or three benzene rings in the evolved products, as shown in Scheme 4, and this is the same both in nitrogen and in air.

Scrutinizing the results of the GC/MS and the LC/MS for the higher molecular weights, it can be seen that the relative
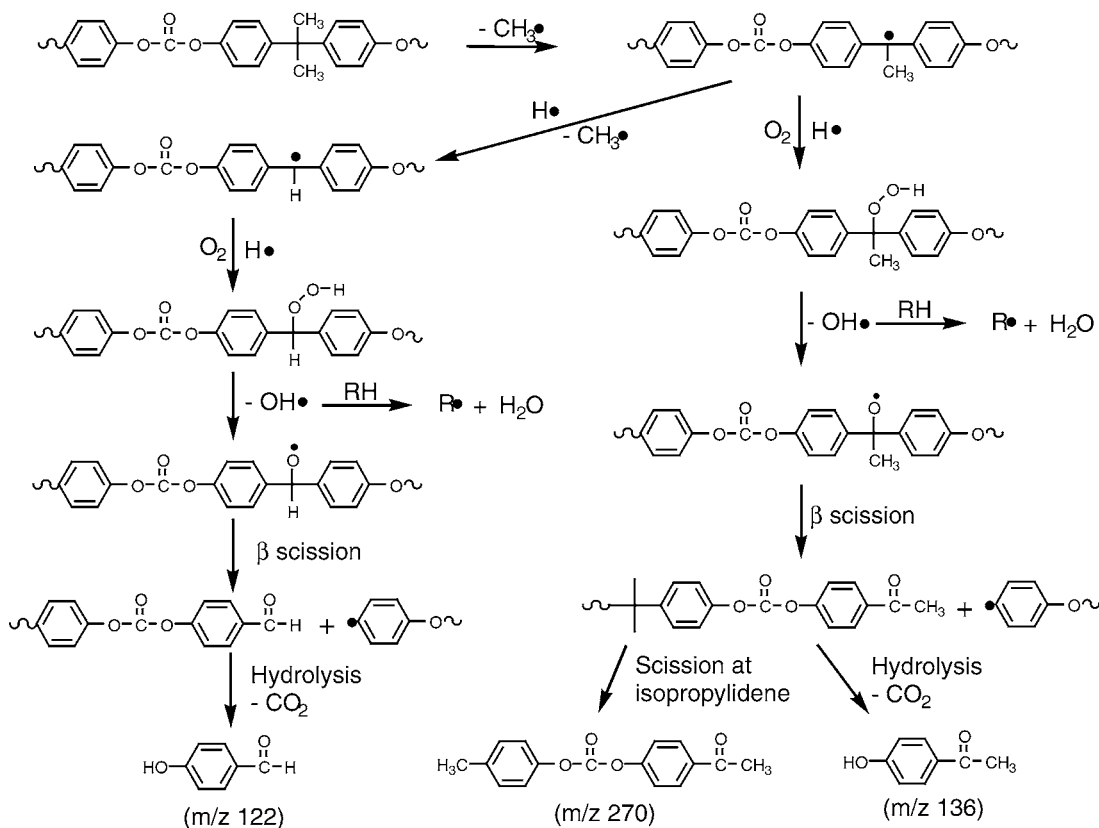
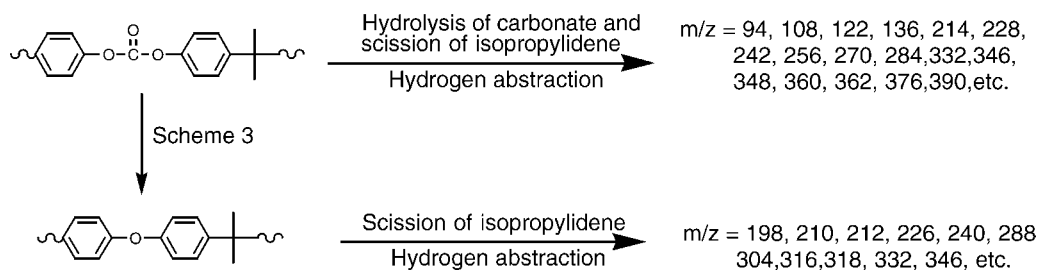Scheme 1.

Scheme 2.

Scheme 3.
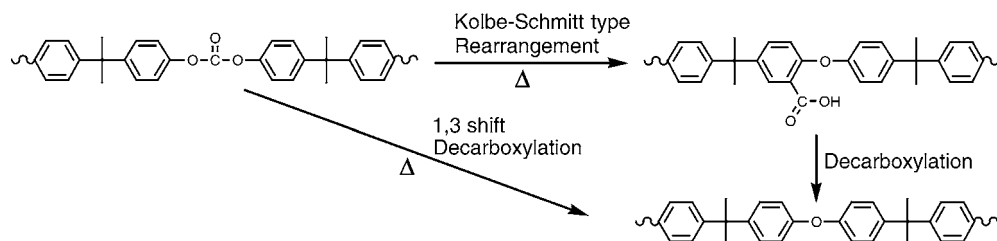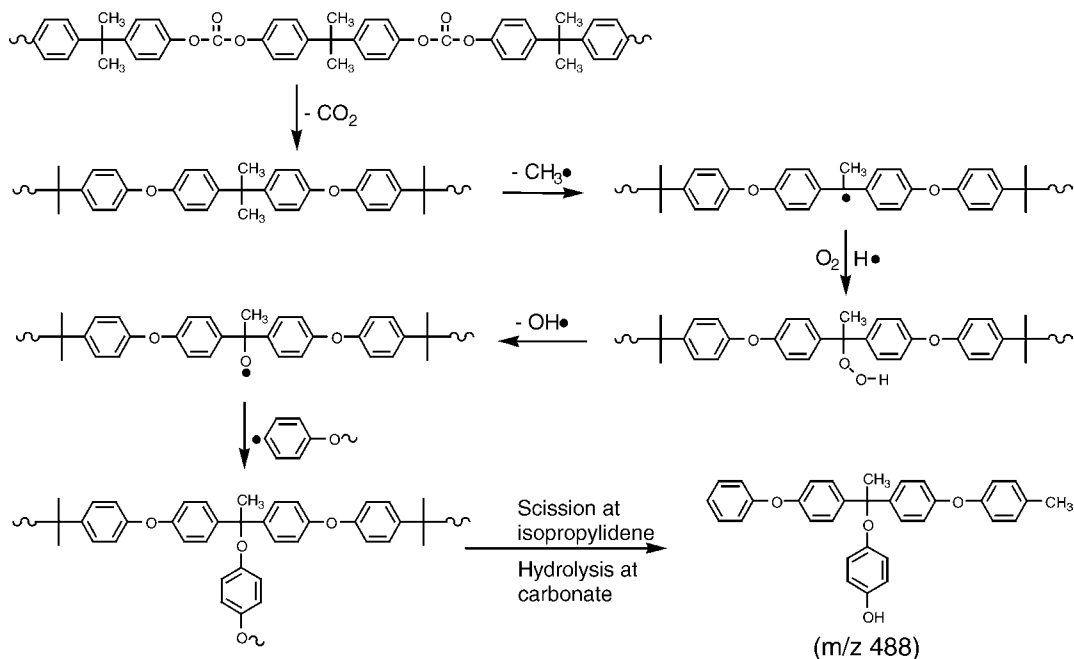
intensity of ether compounds and the number of assigned linear structures are reduced, but branched structures are increased in air. It is speculated that the intermediate surface char formed in the beginning stage of degradation, noted in Scheme 2, assists the formation of branched structures, since this layer may act as a barrier and prevent the evolution of degraded products and give more opportunity for radical recombination reactions leading to branched structures.

It is thought that the 1,1′-diphenylethane skeleton is important in the branched structures. The radical of 1,1′-

diphenylethane produced via methyl scission is quite stable, so it is quite possible to react with other radicals, such as para alkyl substituted phenol radicals in the condensed phase of degrading polycarbonate, as shown in Scheme 5.

3.5. Comparison of these results with previous work

There has not been much work done on the degradation of PC in air. Lee has proposed that hydrogen cleavage from the isopropylidene linkage occurred, followed by alkyl rearrangement producing a tertiary radical [5]. Montaudo et al.
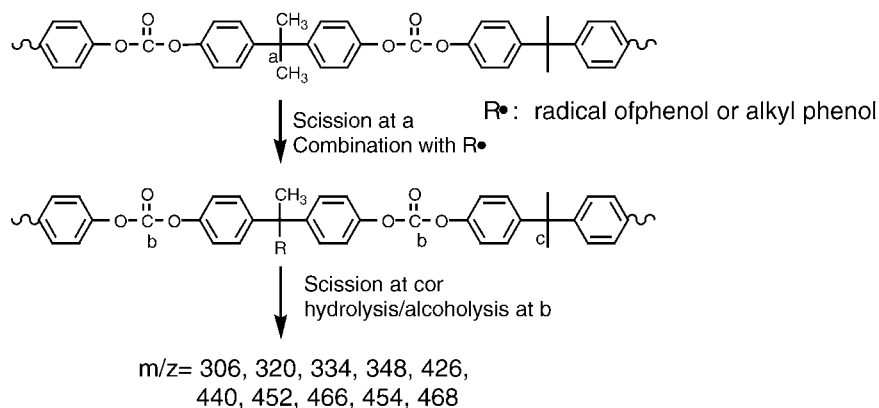
Scheme 4.

Scheme 5.

studied the soluble fraction of solid residues of degraded PC in air, and assigned ketones such as *p*-hydroxybenzophenone via peroxide formation followed by rearrangement [18]. In this study, it has been shown that the initiation of the degradation is through the cleavage of a carbon–carbon bond in the isopropylidene group, followed by reaction with oxygen and the formation of a hydroperoxide. This is completely different from the scheme proposed by earlier authors and is supported by the bond energies. After the initiation of the degradation, the reaction proceeds in the same way as in nitrogen and following a similar pathway to that proposed by Lee [5] and McNeill [9,10]. This means that the presence of oxygen does not effect the main degradation pathway, in agreement with the ideas of Cullis et al. [20], but there is an oxygen effect in the initiation of the degradation. It is likely that the surface char layer which is formed via radical recombination of alkoxy radical in the initiation step acts as barrier during the main mass loss region and, as a result, the mass loss rate is decreases in air.

4. Conclusions

Through the use of TGA/FTIR and chromatography coupled with mass spectrometry, the significant evolved products have been identified for the degradation in air of bisphenol A polycarbonate end-capped with *t*-butyl phenol. In the main degradation region, the thermal degradation in air is very similar to that in nitrogen; the degradation pathways of polycarbonate are chain scission of the isopropylidene linkage, following the order of the bond dissociation energies, and hydrolysis/alcoholysis of the carbonate linkage. It appears that oxygen encourages the branching and cross-linking as well as radical formation via the formation of peroxides. These peroxides undergo further dissociations and radical combinations, which produce aldehydes, ketones and branched structures in the initial mass loss region. Since the oxygen mainly affects the surface of degrading polymers, the differences are mainly observed in the beginning stage of degradation. Poly-

carbonate is one of the good char-forming polymers. Thus, it can be speculated that the reaction between the surface of the degrading polymer and oxygen in air accelerates the formation of an intermediate char on the surface. Due to this insulating layer, there is increased opportunity for radical recombination reactions in the condensed phase. Thus, even though the mass loss begins earlier, a slower mass loss rate is observed.

Acknowledgement

References

[1] D.W. van Krevelen, Polymer 16 (1975) 615.
[2] J. Green, J. Fire Sci. 9 (1991) 285.
[3] J. Green, J. Fire Sci. 12 (1994) 388.
[4] C.A. Wilkie, in: G.L. Nelson (Ed.), Fire and polymers, ACS Symposium Series 425 (1990) 178.
[5] L.H. Lee, J. Polym. Sci. 2 (1964) 2859.
[6] A. Davis, J.H. Golden, J. Gas. Chromatogr. 5 (1967) 81.
[7] A. Davis, J.H. Golden, Macromol. Chem. 110 (1967) 180.
[8] A. Davis, J.H. Golden, J. Macromol. Sci. Rev. Macromol. Chem. C3 (1968) 49.
[9] I.C. McNeill, A. Rincon, Polym. Degrad. Stab. 39 (1993) 13.
[10] I.C. McNeill, A. Rincon, Polym. Degrad. Stab. 31 (1991) 163.
[11] A. Ballistreri, G. Montaudo, C. Puglisi, E. Scamporrino, D. Vitalini, S. Cucinella, J. Polym. Sci., Polym. Chem. Ed. 26 (1988) 2113.
[12] G. Montaudo, C. Puglisi, Polym. Degrad. Stab. 37 (1992) 91.
[13] C. Puglisi, L. Sturiale, G. Montaudo, Macromolecules 32 (1999) 2194.
[14] C. Puglisi, F. Samperi, S. Carroccio, G. Montaudo, Macromolecules 32 (1999) 8821.
[15] G. Montaudo, S. Carroccio, C. Puglisi, Polym. Degrad. Stab. 77 (2002) 137.
[16] G. Montaudo, S. Carroccio, C. Puglish, J. Anal. Appl. Pyrolysis 64 (2002) 229.

[17] B.N. Jang, C.A. Wilkie, Polym. Degrad. Stab, in press.
[18] S. Carroccio, C. Puglisi, G. Montaudo, Macromolecules 35 (2002) 4297.
[19] M.C. Gupta, R.R. Pandey, Makromol. Chem., Macromol. Symp. 27 (1989) 254.
[20] C.F. Cullis, M.M. Hirschler, The Combustion of Organic Polymers, Oxford Press, 1981 (Chapter 3.4.1).
[21] R.M. Asseva, G.E. Zaikov, Combustion of Polymer Materials, New York Press, 1986 (Chapter 2).
[22] T.H. Lowry, K.S. Richardson, Mechanism and Theory in Organic Chemistry, Harper & Row, 1987 (Chapter 9.4–9.5).
[23] C.J. Pouchert, The Aldrich Library of FT-IR Spectra, 1985, p. 44 and 132.
[24] X. Li, M. Huang, Polym. Int. 48 (1999) 387.
[25] J. March, Advanced Organic Chemistry, Wiley Interscience, New York, 1992.
[26] K. Oba, H. Ohtani, S. Tsuge, Polym. Degrad. Stab. 74 (2001) 171.